Electronic Supplementary Material (ESI) for Journal of Materials Chemistry C.

Charge Transfer in the Ag-Polymer-Fullerene System of Organic Solar Cells (OSCs) Observed by Surface-Enhanced Raman Spectroscopy: Donor/Acceptor Concentration-Dependent

Daxin Zhang[1,2,3], Shuo Yang[4], Wenshi Zhao[1,2,3], Lili Yang[3], Yang Liu[3], Maobin Wei[3], Lei Chen*[3] and Jinghai Yang*[3]

[1] *Changchun Institute of Optics, Fine Mechanics and Physics, Chinese Academy of Sciences, Changchun 130033, P.R. China*

[2] *University of Chinese Academy of Sciences, Beijing 100049, P.R. China*

[3] *Key Laboratory of Functional Materials Physics and Chemistry of the Ministry of Education, Jilin Normal University, Changchun 130103, P.R. China*

[4] *College of Science, Changchun University, Changchun 130022, P.R. China*

*To whom correspondence should be addressed.

E-mail: jhyang1@jlnu.edu.cn; chenlei@jlnu.edu.

Experimental

1.1 Materials

Silicon (Si) wafer (100) and soda-lime glass (the thickness of ~ 2 mm) were purchased from Hefei Kejing Material Technology Co., Ltd. The Si wafer and soda-lime glass were cut into pieces with dimensions of 1.0 cm × 1.0 cm and 1.0 cm × 2.0 cm, respectively. Ag with 99.99% purity was purchased from Beijing Tianrui Science and Technology Development Center. P3HT (regioregularity ≥ 90.0%, MW=50,000 g/mol) and PCBM (purity ≥ 99%, MW=910.88 g/mol) were Shanghai Aladdin Biochemical Technology Co., LTD. H_2O_2 (30%) and NH_4OH (25%) were all purchased from National Pharmaceutical Chemical Reagent Co., Ltd. Chlorobenzene was purchased from Sinopharm Chemical Reagent Co., Ltd. They were of the highest purity available, and the chemical reagents were used without further purification. Deionized ultrapure water (18.25 MΩ•cm^{-1}) was used throughout the present study.

1.2 Characterization of the films

Morphology and microstructure images of the samples were obtained using a JEOL 6500F scanning electron microscope (SEM) and a MFP-3D-BIO atomic force microscopy (AFM). The energy dispersive spectrometry (EDS) was also performed by SEM linked with an Oxford Instruments X-ray analysis system. Ultraviolet-visible (UV–Vis) absorbance spectra were obtained using a Shimadzu UV-3600 spectrometer. The X-ray diffraction (XRD) measurement was performed on a Japan Rigaku D/max-ga X-ray diffractometer with Cu Kα radiation (λ=1.5418 Å) at room temperature. The step size (2θ) is 0.01°. Hall measurements were performed with van der Pauw configuration by Lake Shore 7704A at room temperature. All Raman spectra were obtained using a confocal Renishaw Raman system 2000 model microscope spectrometer with a 514.5 nm excitation. The optical power of 20 mW, an acquisition time of 30 s, and acquisition time 2 s were used for the excitation conditions.

1.3 Preparation of the Si wafers and soda-lime glasses

Si wafers and soda-lime glasses were heated to 300 ℃ and kept for 5 minutes in the mixed solution (deionized ultrapure $H_2O/H_2O_2/NH_4OH$ = 6:2:1, v/v).[1] After

cooling to room temperature, they were washed by ultrasonic using deionized ultrapure water and alcohol alternately. Finally, they were stored in deionized ultrapure water for later use.

1.4 Preparation of the Ag substrates

The Ag substrates were fabricated by a magnetron sputtering system (ATC 1800-F, USA AJA) at the sputtering power of 10 W for 60 s.[2] The thickness is ~ 10 nm measured by Profile-system.

1.5 Fabrication of the Ag/P3HT/PCBM thin films

The Ag/P3HT/PCBM thin films were fabricated by a growth and nucleation process described as follows. Firstly, 0.1 mM P3HT and 0.01 M PCBM solution were prepared with chlorobenzene as the solvent and oscillated for 1 h until completely dissolved. Then, 0.1 mM P3HT and 0.01 M PCBM precursor were diluted to various concentrations (0.01 - 0.0001 mM) and (1 - 0.01 mM) precursor, respectively. Secondly, 0.01 mM P3HT precursor solution was dropped on the Si wafers/Ag films. Then, they were covered to generate the Si wafers/Ag/P3HT (0.01 mM) films. After 6 h, various concentrations PCBM precursor solution was dropped on the Si wafers/Ag/P3HT (0.01 mM).[3-4] Finally, the Ag/P3HT (0.01 mM)/PCBM (10 - 0.01 mM) films were achieved as the solvent slowly evaporated in the air at room temperature. Likewise, the Ag/PCBM (10 mM)/P3HT (0.1- 0.0001 mM) film were achieved. It grew on the soda-lime glasses in the same way as the Si wafers. The precursor solution is 50 μL dripping on the Si wafers, and the precursor solution is 100 μL dripping on the soda-lime glasses.

Surface morphology characterization

Ag/PCBM/P3HT heterostructures with controlled concentration of the P3HT (0.1–0.0001 mM) were synthesized in Figure S1. Figure S1(a-e) were the SEM images of the Ag/PCBM (10 mM) and the Ag/PCBM (10 mM)/P3HT (0.1 - 0.0001 mM). The EDS mapping showed uniform elemental distributions of silver (Ag) from Ag substrate, sulfur (S) from the P3HT and oxygen (O) from PCBM and oxidized part in

the Figure S1(a1-e4). Due to the high regularity of P3HT, there are no obvious irregular nanostripes in the thin films. The surface of pure Ag/PCBM (10 mM) film with a thickness of ~ 614.3 nm showed relatively smooth. However, the surface covered with the P3HT gets rough, and the thickness is thinner, approximately 388.1 nm thick. With additionally decreasing P3HT concentration from 0.1 to 0.0001 mM, Ag nanoparticles on the substrate appear more and more clearly, just as the detected Ag element gradually decreases in the Figure S1(b1-e1) and the thicknesses decrease from 388.1 to 172.5 nm. The detected S element from P3HT gradually decreases in EDS, while the O and C elements decrease with P3HT concentrations. The insets are optical photographs of the samples, which show significant colour changes and film information. According to the SEM images and optical photographs, the growth of Ag/PCBM/P3HT (0.01 mM) film is homogeneous. Figure S2(a) is the three dimensional (3D) height sensor AFM image of Ag/PCBM/P3HT (0.01 mM), in which the root mean square (RMS) surface roughness is ~ 0.3 nm, showing that the surface is extremely homogeneous.[5-6]

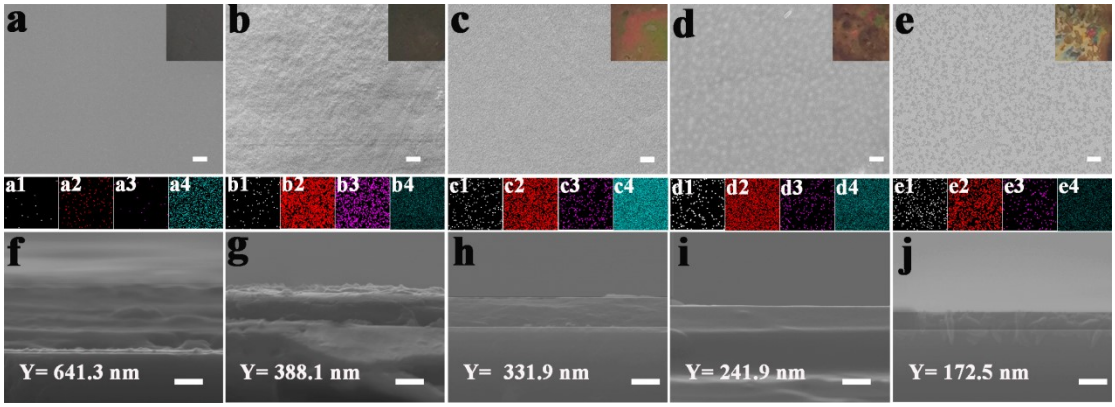

Figure S1. (a-e) The scanning electron microscopy (SEM) of the Ag/PCBM (10 mM) (a), the Ag/PCBM (10 mM)/P3HT (0.1-0.0001 mM) (=1, v/v) (b-e). The insets are optical photographs of the corresponding samples. The small red circles represent Ag nanoparticles and the small yellow lines represent nanostripes. (a1-e4) The EDS mapping of elemental distributions: silver (Ag) (white color), oxygen (O) (red color), sulfur (S) (pink color) and carbon (C) (cyan color). (f-j) The cross section SEM of the Ag/P3HT (0.1 mM) (f), the Ag/P3HT (0.01 mM)/PCBM (10-0.01 mM) (=1, v/v) (g-j), corresponding to the SEM. The Y is the thicknesses of the samples, which is ± 0.1

nm. The scale bars correspond to 250 nm.

To confirm the variation of crystallinity or internal morphology change in P3HT and PCBM, we need further characterization of prepared polymer thin film samples by XRD in the Figure S2 b. Like the Ag/P3HT/PCBM system, the height of the diffraction peak at 2θ=5.3°drops and is even unobserved because of the decreasing concentration of P3HT. With the reduction of P3HT, diffraction peaks of the films are gradually similar to the PCBM, whereas the height of and diffraction angle of the Ag (111) keeps constant because of the stability of Ag. This means that the Ag substrate has high stability and do not affected by crystallization of P3HT and aggregation of PCBM.[6,7]

Optical characterization

UV-vis absorbance spectra of the Ag/PCBM/P3HT (0.1-0.0001 mM) thin films show in the Figure S2 c. A representing Ag/P3HT (0.1 mM) thin film has a strong light absorbance in the visible region, whereas representing Ag/PCBM (10 mM) thin film mainly absorbs light in the near UV region. When the Ag/PCBM film was covered by P3HT (0.1 mM), the light absorbance is similarly to the Ag/P3HT (0.1 mM) thin film because of the excessive light absorbance of P3HT. As the decrease of P3HT, the characteristic absorbance peaks of P3HT gradually disappear, and absorbance peaks intensity of PCBM at ~ 450 nm gradually decreases. However, the obvious peak at ~ 350 nm assigned to the $^1T_{1u}$-^1A_g electron transitions in C_{60} shows a weak redshift, and the half-peak width is increasing.[8] This is mainly because the reduction of P3HT caused an increase in the aggregation of PCBMs. The absorbance spectra and diffraction peaks of the blend films are similar to the pristine P3HT with the decrease of P3HT, but the intensity is lower due to the reduction of the P3HT, as shown in the Figures S2 b and c.

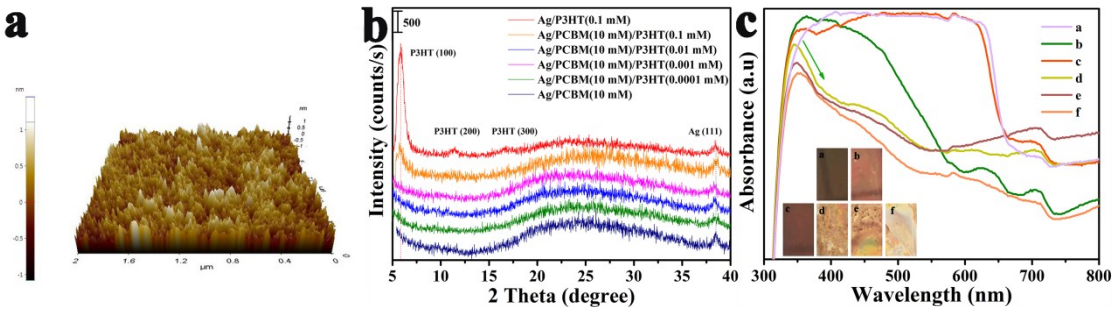

Figure S2. (a) The three dimensional (3D) height sensor AFM image of Ag/PCBM/P3HT (0.01 mM), and the root mean squard (RMS) surface roughness is ~ 0.3 nm. (b) XRD pattern of the thin films. (c) UV-vis absorbance spectra of thin films: Ag/P3HT (0.1 mM)(a), Ag/PCBM (10 mM) (b), Ag/PCBM (10 mM)/P3HT (0.1-0.0001 mM)(c-f).

Carrier density characterization

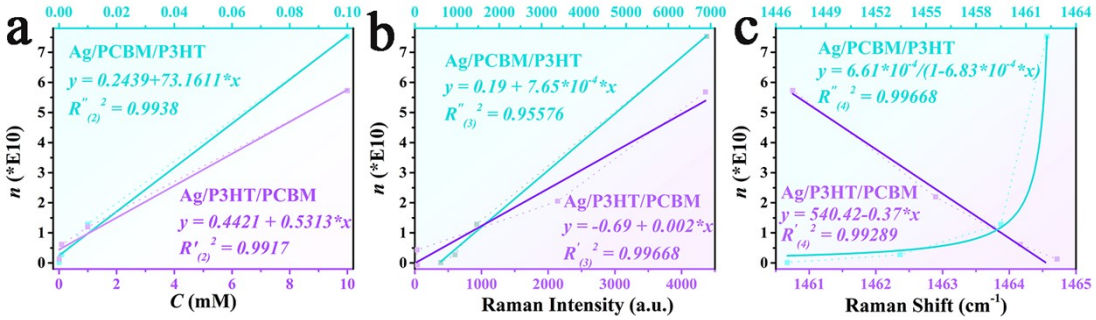

Figure S3. (a) The fitting curves of the carrier density (n) and concentrations (C) respectively. (b) The fitting curves of n and Raman intensity (I) respectively. (c) The fitting curves of n and Raman shift (v) respectively. (Cyan represents the Ag/PCBM/P3HT(0.1-0.0001 mM), and purple represents the Ag/P3HT/PCBM (10-0.01 mM)).

Carrier density was obtained using Hall tests and fitted them to donor/acceptor concentrations, Raman shifts and Raman intensities. As shown in Figure S3 a, the carrier density is proportional to the acceptor/donor concentrations, and $R^2 > 99\%$. As the acceptor/donor concentrations decrease, carrier density also decreases. In the Ag/PCBM/P3HT system, the slope of the fitting equation is higher, indicating that the donor has greater influence on the carrier density than the acceptor. This is mainly

due to the high carrier density of the donor in Table S2 and 3. Carrier density is regulated by the donor/acceptor concentrations. There are obviously different phenomena in the SERS affected by carrier density, on the one hand is Raman shift, on the other hand is Raman intensity. In Figure S3 b, carrier density increases the Raman intensity, and the main contribution comes from the electromagnetic field enhancement and charge transfer (CT). With the increase of carrier density, the spacing between molecules decreases, the magnetic moment increases and the electromagnetic field increases. In Figure S3 c, carrier density with an increased acceptor concentration causes a blue shift, while carrier density with an increased donor concentration causes a red shift. Here, the influence of CT between donor and acceptor in the system is considered. The concentrations of donor and acceptor increase the CT in different paths. Detailed analysis is mentioned in the manuscript.

Table S1. Wavenumbers, assignments and sample of the bands at 514.5 nm excitation wavelength in the SERS spectra of the pure P3HT and PCBM. Raman shift is ± 0.1 cm^{-1}.[9]

Wavenumbers (cm^{-1})	Assignments	sample
709.1	$H_g(3)$ of the C_{60}	PCBM
724.6	antisymmetric ring *ν* (C_α –S–C_α)	P3HT
1003.0	*ν* (C_β –C_{alkyl})	P3HT
1088.4	*γ* (C–H)	P3HT
1169.1	symmetric ν (C_α –C_α)	P3HT
1184.8	*ν* (C_α –C_α)	P3HT
1205.2	*ν* (C_β –H)	P3HT
1377.3	skeletal *ν* (C_β –C_β)	P3HT
1425.0	$H_g(7)$ of the C_{60}	PCBM
1444.0	symmetric *ν* (C_α = C_β)	P3HT
1460.7	$A_g(2)$ of the C_{60}	PCBM
1514.2	antisymmetric *ν* (C_α = C_β)	P3HT
1573.6	$H_g(8)$ of the C_{60}	PCBM

[a]*ν*, stretching; *γ*, bending. For ring vibrations, the corresponding vibrational modes of benzene and the symmetry species under C_{2v} symmetry are indicated.

Table S2. The Hall element's test data for samples in the Ag/P3HT(0.01 mM)/PCBM(10–0.1 mM) system, as well as the Ag/P3HT (0.1 mM).

Sample	Average	n	Δn_{max}
Ag/P3HT(0.01 mM)	1.6011E+11	3.8681E+11 9.5400E+10 1.0242E+11	4.6617E+10
Ag/P3HT(0.01 mM)/PCBM(10 mM)	5.7322E+10	5.5803E+10 4.6398E+10 2.8865E+11 6.5810E+9	2.8435E+11
Ag/P3HT(0.01 mM)/PCBM(1 mM)	2.1966E+10	4.2968E+9 2.6619E+9 1.2594E+9 3.3604E+9	7.9325E+10
Ag/P3HT(0.01 mM)/PCBM(0.1 mM)	6.1441E+9	8.0584E+10 1.0860E+9 1.7934E+9 1.1133E+10	1.0343E+10
Ag/P3HT(0.01 mM)/PCBM(0.1 mM)	1.2833E+9	7.8983E+8 1.8589E+9 5.3268E+8 1.0964E+9 1.6444E+9	1.1117E+10

Table S3. The Hall element's test data for samples in the Ag/PCBM(10 mM)/P3HT(0.1 - 0.0001 mM) system, as well as the Ag/PCBM (10 mM).

Sample	Average	n	Δn_{max}
Ag/PCBM(10 mM)	1.6594E+9	3.8749E+9	2.4575E+9
		1.6861E+9	
		1.7191E+9	
Ag/PCBM(10 mM)/P3HT(0.1 mM)	7.5295E+10	2.8450E+9	3.9490E+10
		1.3620E+10	
		1.6191E+11	
		1.2241E+10	
		1.1341E+11	
Ag/PCBM(10 mM)/P3HT(0.01 mM)	1.0955E+10	1.0824E+9	2.7394E+10
		2.4158E+9	
		4.1838E+9	
		2.9810E+10	
Ag/PCBM(10 mM)/P3HT(0.001 mM)	2.7120E+9	9.0533E+7	5.6951E+9
		5.7856E+9	
		4.3882E+9	
Ag/PCBM(10 mM)/P3HT(0.0001 mM)	1.5482E+8	5.8368E+8	1.7138E+8
		2.4337E+7	
		2.4854E+8	
		8.7507E+7	
		2.5889E+8	

References:

1 N. Ma, X. Y. Zhang, W. Fan, S. Guo, Y. Zhang, Y. Liu, L. Chen and Y. M. Jung, *Spectrochim. Acta A* 2019, **219,** 147-153.

2 D. Zhang, S. Yang, X.-Y. Zhang, N. Ma, B. Han, W. Zhao, S. Chi, Y. Liu, J. Yang and L. Chen, *Spectrochim. Acta A* 2020, **238,** 118430.

3 J. Xing, Y. Zou, C. Zhao, Z. Yu, Y. Shan, W. Kong, X. Zheng, X. Li, W. Yu and C. Guo, *Mater. Today Phys.* 2020, **14,** 7.

4 W. Yu, F. Li, L. Yu, M. R. Niazi, Y. Zou, D. Corzo, A. Basu, C. Ma, S. Dey, M. L. Tietze, U. Buttner, X. Wang, Z. Wang, M. N. Hedhili, C. Guo, T. Wu and A. Amassian, *Nat. Commun.* 2018, **9,** 5354.

5 W. C. Tsoi, D. T. James, J. S. Kim, P. G. Nicholson, C. E. Murphy, D. D. Bradley, J. Nelson and J. S. Kim, *J. Am. Chem. Soc.* 2011, **133,** 9834-43.

6 Y. Kim, S. Cook, S. M. Tuladhar, S. A. Choulis, J. Nelson, J. R. Durrant, D. D. C. Bradley, M. Giles, I. McCulloch, C. S. Ha and M. Ree, *Nat. Mater.* 2006, **5**, 197-203.

7 T. Erb, U. Zhokhavets, G. Gobsch, S. Raleva, B. Stühn, P. Schilinsky, C. Waldauf and C. J. Brabec, *Adv. Funct. Mater.* 2005, **15,** 1193-1196.

8 T.-A. Chen, X. Wu and R. D. Rieke, *J. Am. Chem. Soc.* 1995, **117,** 233.

9 H. Kuzmany, M. Matus, B. Burger and J. Winter, *Adv. Mater.* 1994, **6,** 731-745.